Int. J. Heat Mass Transfer. Vol. 33, No. 3, pp. 401–408, 1990
Printed in Great Britain

0017–9310/90 $3.00 + 0.00

Unsteady conjugate heat transfer from a translating fluid sphere at moderate Reynolds numbers

D. L. R. OLIVER
Department of Mechanical Engineering, University of Toledo, Toledo, OH 43604, U.S.A.

and

J. N. CHUNG
Department of Mechanical and Materials Engineering, Washington State University, Pullman, WA 99164-2920, U.S.A.

(*Received* 10 *March* 1988 *and in final form* 16 *May* 1989)

Abstract—The conjugate unsteady heat transfer between a translating droplet and its surrounding fluid at moderate Reynolds number is numerically investigated. The energy equation is solved by the ADI finite difference method with fluid motions inside and outside the droplet simulated by a series-truncation spectral method. The range of Reynolds numbers investigated is between 0 and 50. The ratios of viscosity and thermal conductivity between a droplet and its ambient flow range from 0 to 10^7 and 0.01 to 3, respectively. It was found that by increasing the Reynolds number, the predicted rate of heat transfer is significantly increased for fluid spheres as a result of increased fluid motions both inside and outside the droplet. On the other hand, the transfer rate for a solid sphere is much less sensitive to the Reynolds number than are the fluid spheres. For a gas bubble, any increase in the Reynolds number only increases the amplitude and frequency of the fluctuations in the Nusselt number and the steady-state Nusselt number is nearly independent of the Reynolds number.

1. INTRODUCTION

THE PHENOMENA of transport of heat and mass between a translating droplet and its surrounding fluid have been investigated intensively due to a wide range of industrial and scientific applications. As explained in ref. [1], the problem is classified as 'external' or 'internal' if the transfer resistance is assumed negligible inside the droplet as compared to that of the continuous phase or vice versa. A literature review of these two extreme cases was given in ref. [1] and will not be repeated here.

In many applications, the transport should be treated as a conjugate process where resistances of both the dispersed and the continuous phases are comparable to each other, therefore, both should be retained in the analysis. For conjugate problems the majority of the work in the literature is concerned with droplets or spheres in the creeping flow regime. Cooper [2] developed an analytical solution of the temperature fields with various combinations of thermal properties for heat transfer to a sphere at very low Peclet numbers.

Abramzon and Borde [3] used a finite difference method to study the conjugate heat transfer from a droplet in creeping motion. Both the fluid and the solid spheres were included in the analysis. Their work provides a comprehensive understanding of the transport mechanisms. However, they only addressed systems with identical thermal properties in both phases that do not have application values in most realistic systems.

The work of Abramzon and Borde [3] was extended in ref. [1] to include variable ratios of heat capacities. But in ref. [1], the ratio of thermal diffusivities is restricted to unity and also the flow is in the creeping regime. It was found that the temperature profile (as made dimensionless by the difference between the temporal bulk temperature of the droplet and the ambient temperature) asymptotically approaches a steady-state value that is independent of the initial temperature profile in the droplet. As a result of this asymptotic behavior of the dimensionless temperature profile, the Nusselt number also asymptotically approaches a steady-state value.

For high Reynolds number flows, Chao [4] used boundary layer assumptions to estimate the conjugate heat transfer rates from a droplet. Due to the elliptic nature of the interior region, such boundary layer solutions will be inaccurate except at small times.

Based on the above literature review we realize that there is a need to fill the gap due to the lack of work for moderate Reynolds number flows in conjugate heat transfer of a translating droplet. Closed-form analytical solutions are available for both low and high Reynolds number flows, whereas numerical com-

NOMENCLATURE

a	radius of the sphere or droplet
A	ratio of thermal diffusivities, α_1/α_2
B	ratio of thermal conductivity, k_1/k_2
c	specific heat
F_n	radial function for the stream function
Fo_2	Fourier number, $\alpha_2 t/a^2$
H	ratio of volumetric heat capacities, $\rho_1 c_1/\rho_2 c_2$
k	thermal conductivity
Nu	Nusselt number
Pe_2	Peclet number based on continuous phase properties, $2aU_\infty/\alpha_2$
P_n	Legendre polynomial of order n
r	dimensionless radial coordinate, R/a
R	radial coordinate
Re_1	Reynolds number based on dispersed phase properties, $2\rho_1 aU_\infty/\mu_1$
Re_2	Reynolds number based on continuous phase properties, $2\rho_\infty aU_\infty/\mu_\infty$
t	time
T	temperature
u	dimensionless radial velocity, U/U_∞
U_∞	velocity of the sphere
v	dimensionless tangential velocity, V/U_∞
W	Zr
X	ratio of dynamic viscosities, μ_1/μ_2
Z	dimensionless temperature, $(T-T_\infty)/(T_{1,0}-T_\infty)$.

Greek symbols

α	thermal diffusivity
η	$1/r$
θ	tangential coordinate
μ	dynamic viscosity
ρ	density
$\tau_{r\theta}$	tangential shear stress
ψ	dimensionless stream function.

Subscripts

1	dispersed phase
2	continuous phase
asy	asymptotic
b	bulk
ext	exterior of the droplet
int	interior of the droplet
0	initial condition
∞	free stream.

putations seem to be the only tractable means for moderate Reynolds number flows for a translating droplet. In this study, our previous work [1] is expanded to moderate Reynolds number flows. The flow field was simulated by a series-truncation spectral method and the decoupled energy equation was solved again by the ADI method.

2. MATHEMATICAL MODEL

We consider a fluid sphere of radius a, initially at a uniform temperature T_0 and falling at a constant velocity U_∞ in another immiscible fluid of infinite extent. At time $t = 0$ the temperature of the continuous phase fluid undergoes a step change from T_0 to T_∞. It is the objective of this study to examine the transient heat transfer rates between the fluid sphere and its ambient fluid. The following assumptions are used in the analysis.

(1) The size and shape of the fluid sphere stay constant during the transient and the two fluids are non-reacting.

(2) Constant properties and negligible dissipations are assumed. Therefore, the flow analysis is decoupled from the energy equation. Buoyancy driven flows are also neglected.

(3) There is no surface active agent and the flows are fully developed and steady both inside and outside the sphere.

(4) Absence of oscillation and rotation of the fluid sphere is assumed.

(5) The maximum Reynolds number of the fluid sphere, $Re_2 = 2\rho_\infty U_\infty a/\mu_\infty$, is moderate such that the flows are laminar.

The schematic of the physical model and coordinate system are shown in Fig. 1.

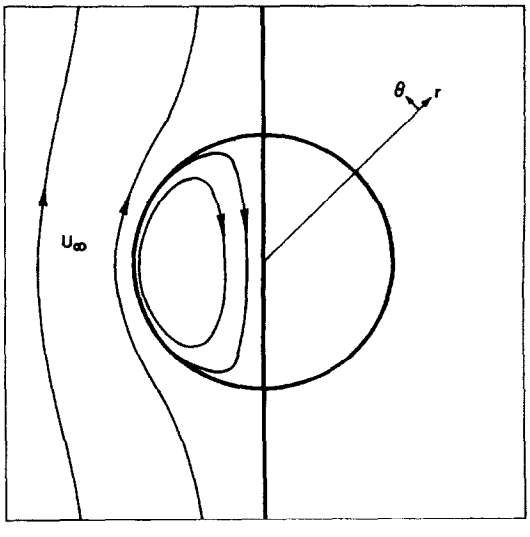

FIG. 1. Schematic of the coordinate system and typical flow lines for a translating fluid sphere.

2.1. *Flow fields analysis*

In terms of the dimensionless stream function, ψ, the dimensionless radial and tangential velocities are given by

$$u = \frac{1}{r^2 \sin\theta}\frac{\partial\psi}{\partial\theta} \tag{1}$$

$$v = \frac{-1}{r\sin\theta}\frac{\partial\psi}{\partial r}. \tag{2}$$

In the above, the stream function is made dimensionless with $U_\infty a^2$, the velocities are made dimensionless with the free stream velocity U_∞, and the radial coordinate r is made dimensionless with a. The dimensionless equation of motion in terms of the stream function is

$$E^4\psi = \frac{Re}{2}\sin\theta\left[\frac{\partial\psi}{\partial r}\frac{\partial}{\partial\theta}\left(\frac{E^2\psi}{r^2\sin^2\theta}\right) - \frac{\partial\psi}{\partial\theta}\frac{\partial}{\partial r}\left(\frac{E^2\psi}{r^2\sin^2\theta}\right)\right] \tag{3}$$

with

$$E^2 = \frac{\partial^2}{\partial r^2} + \frac{\sin\theta}{r^2}\frac{\partial}{\partial\theta}\left(\frac{1}{\sin\theta}\frac{\partial}{\partial\theta}\right).$$

Equation (3) is valid for both the fluid sphere and its ambient flow. The Reynolds number should be $Re_1 = 2\rho_1 U_\infty a/\mu_1$ for flow in the fluid sphere and $Re_2 = 2\rho_\infty U_\infty a/\mu_\infty$ for ambient flow. The boundary conditions to be satisfied by equation (3) are:

(a) at the axis symmetry ($\theta = 0, \pi$)

$$\frac{\partial\psi_1}{\partial\theta} = 0 \quad (u \text{ is finite}) \tag{4}$$

$$\psi_1 = 0 \quad (\text{reference value}); \tag{5}$$

(b) at the interface ($r = 1$)

$$\frac{\partial\psi_1}{\partial r} = \frac{\partial\psi_2}{\partial r} \quad (\text{no slip}) \tag{6}$$

$$\tau_{r\theta_1} = \tau_{r\theta_2} \quad (\text{continuity of shear stress}) \tag{7}$$

$$\psi_1 = \psi_2 = 0; \tag{8}$$

(c) at the free stream condition ($r \to \infty$)

$$\psi_2 = \tfrac{1}{2}r^2\sin^2\theta. \tag{9}$$

The series-truncation spectral method originally proposed by Van Dyke [5] is used to solve the fluid flow problem. The basic procedure of this method is that we define the stream function as an infinite series of Legendre polynomials P_n with corresponding radial function F_n

$$\psi = \sum_{n=1}^{\infty} F_n(r)\int_{\bar{z}}^{1} P_n(t)\,dt; \quad \bar{z} = \cos\theta. \tag{10}$$

Thus, from here

$$u = \sum_{n=1}^{\infty}\frac{F_n(r)}{r^2}P_n(\bar{z}) \tag{11}$$

$$v = \sum_{n=1}^{\infty}\frac{-F_n'(r)}{r}\frac{P_n^1(\bar{z})}{n(n+1)}. \tag{12}$$

With equation (10), the equation of motion (equation (3)) is transformed into a series of ordinary nonlinear differential equations. The series of ordinary differential equations is then truncated properly and solved by a cubic finite-element scheme. Details of the solution procedure and flow results for $0.5 < Re_2 < 50$ are given in ref. [6].

2.2. *Conjugate heat transfer analysis*

The appropriate dimensionless energy equation for the fluid sphere is

$$\frac{1}{A}\frac{\partial Z}{\partial Fo_2} + \frac{1}{A}\frac{Pe_2}{2}\left[u\frac{\partial Z}{\partial r} + \frac{v}{r}\frac{\partial Z}{\partial\theta}\right] = \frac{\partial^2 Z}{\partial r^2} + \frac{2}{r}\frac{\partial Z}{\partial r} + \frac{1}{r^2}\cot\theta\frac{2Z}{\partial\theta} + \frac{1}{r^2}\frac{\partial^2 Z}{\partial\theta^2} \tag{13}$$

where Z is the dimensionless temperature based on the initial temperature difference

$$Z = (T - T_\infty)/(T_{1,0} - T_\infty). \tag{14}$$

The dimensionless parameters: Fo_2 (Fourier number) $= \alpha_2 t/a^2$ and Pe_2 (Peclet number) $= 2aU_\infty/\alpha_2$. A is the ratio of internal thermal diffusivity (α_1) to external thermal diffusivity (α_2).

Initial conditions

$$Z(r, \theta, Fo_2 = 0) = 1, \quad 0 < r < 1 \tag{15}$$

$$Z(r, \theta, Fo_2 = 0) = 0, \quad 1 < r < \infty. \tag{16}$$

Boundary conditions

$$B\frac{\partial Z_1}{\partial r} = \frac{\partial Z_2}{\partial r}, \; r = 1 \quad (\text{continuity of heat flux})$$

$$B = k_1/k_2 \quad (\text{ratio of thermal conductivities}) \tag{17}$$

$$Z(r, \theta, Fo_2) = 0, \quad r \to \infty \tag{18}$$

$$\frac{\partial Z}{\partial\theta} = 0, \quad \theta = 0 \text{ and } \pi \tag{19}$$

$$Z(r, \theta, Fo) = \text{finite}, \quad r = 0. \tag{20}$$

3. SOLUTION PROCEDURE

At the droplet center ($r = 0$) the boundary condition on $Z(r = 0)$ is imposed by defining a new variable for the interior region: $W = Zr$. Thus the boundary condition at the droplet center becomes

$$W(r = 0, t) = 0. \tag{21}$$

The transformed energy equation for the droplet phase is

$$A^{-1}\frac{\partial W}{\partial Fo_2}+\frac{Pe_2}{2A}\left[u\left(\frac{\partial W}{\partial r}-\frac{W}{r}\right)+\frac{v}{r}\frac{\partial W}{\partial \theta}\right]$$
$$=\frac{\partial^2 W}{\partial r^2}+\frac{1}{r^2}\cot\theta\frac{\partial W}{\partial \theta}+\frac{1}{r^2}\frac{\partial^2 W}{\partial \theta^2}. \quad (22)$$

In the exterior region, a high density of nodes are used near the interface, with fewer nodes near the free stream. This is accomplished by using the transformation $\eta = 1/r$. This transformation appears to be a better choice than the usual transformation $\xi = \ln(r)$, in that the former transformation allows one to obtain a close spacing near the interface, without regard to the exact location at which the free stream conditions are imposed, since $\eta = 0$ is a 'point at infinity'. The transformation $\eta = 1/r$ also needs fewer total nodal points for comparable grid spacing at the interface. The transformed energy equation for the continuous phase is given by

$$\frac{\partial Z}{\partial Fo_2}+\frac{Pe_2}{2}\left[-\eta^2 u\frac{\partial Z}{\partial \eta}+\eta v\frac{\partial Z}{\partial \theta}\right]$$
$$=\eta^4\frac{\partial^2 Z}{\partial \eta^2}+\eta^2\cot\theta\frac{\partial Z}{\partial \theta}+\eta^2\frac{\partial^2 Z}{\partial \theta^2}. \quad (23)$$

The step size $\Delta\eta$ is chosen such that $\Delta\eta = \Delta r/(\Delta r+1)$.

For the initial conditions at the interface, a control volume analysis yields the initial interfacial temperature of

$$Z(r=1,\theta,t=0) = Z_2(\eta=1,\theta,0)$$
$$= H/[(1+\Delta r)+H]. \quad (24)$$

Initial conditions for all other points being

$$Z(r,\theta,t=0)=1, \quad 0<r<1 \quad (25)$$

$$Z(\eta,\theta,t=0)=0, \quad 0<\eta<1. \quad (26)$$

The boundary conditions imposed on equations (11) and (12) are

$$W(r=0,t)=0 \quad (27)$$

$$B\left(\frac{\partial W}{\partial r}-\frac{W}{r}\right)+\frac{\partial Z}{\partial \eta}=0 \quad \text{at } r=1,\ \eta=1 \quad (28)$$

$$\frac{\partial W}{\partial \theta}=0, \quad \frac{\partial Z}{\partial \theta}=0, \quad \text{for } \theta=0 \text{ and } \pi \quad (29)$$

$$Z(\eta=0,\theta,t)=0 \quad \text{(free stream condition)}. \quad (30)$$

Equations (22) and (23) were solved with an ADI procedure similar to that used by Abramzon and Borde [3], the primary exceptions are the transformation used in equation (23), and the interfacial boundary condition (equation (28)). It was not found necessary to use any up-wind differencing scheme to model the convective terms, these terms were modeled with central-difference approximations. The discretization for the energy equations (equations (23) and (24)) is identical to those shown in ref. [1] and is skipped here.

When the finite difference energy equations are treated with the normal ADI method, a tridiagonal matrix results everywhere in the computational domain except at the interfacial boundary ($r = 1$) and at the symmetrical boundaries ($\theta = 0$ and π). At these three boundaries the tridiagonal algorithm is modified to account for the additional matrix components which are outside the main three bands. A 41×41 grid was used (i.e. $\Delta r = 1/40$ and $\Delta\theta = \pi/40$). The time step used varied with each simulation, it depends on the Peclet number, the ratio of thermal diffusivities, and the ratio of viscosities. For each simulation the time step was held constant. The time step was not increased with time for two reasons: the system might be unstable if the time step was too large and the 'LU' decompositions of the resulting matrices needed to be recomputed with each change in the time step size.

4. COMPARISONS WITH PREVIOUS INVESTIGATIONS

The Nusselt number will be used to compare the present model with the various special cases cited above and also will be used to present the result of current calculations. The Nusselt number is defined first. The bulk dimensionless temperature is given as

$$Z_b = \frac{3}{2}\int_0^{\pi}\int_0^{r} Zr^2\sin\theta\,dr\,d\theta. \quad (31)$$

The Nusselt number is defined by the relation

$$Nu = \frac{2aQ}{4\pi a^2(T_{1,b}-T_\infty)K_2} \quad (32)$$

which is equivalent to

$$Nu = -\tfrac{2}{3}H\frac{1}{Z_b}\frac{dZ_b}{dFo_2}. \quad (33)$$

One may also approximate the Nusselt number by calculating the flux of heat from the surface of the sphere

$$Nu = \frac{\int_0^{\pi}\left.\frac{\partial Z_2}{\partial \eta}\right|_{\eta=1}\sin\theta\,d\theta}{Z_b}. \quad (34)$$

In numerical computations, equations (32) and (34) may not predict identical Nusselt numbers. As discussed in ref. [1], equation (34) was used to compute all the results of Nusselt number in this paper.

The theory and coding may be partially verified by comparison of the present results with certain previous numerical and experimental investigations. Dennis *et al.* [7] used a similar series truncation method to predict the steady-state Nusselt number for a solid sphere with $Pe_2 = 14.6$ and $Re_2 = 20$. Their analysis predicted a Nusselt number of $Nu = 4.065$. On Fig. 2 the Nusselt number predicted by the present method is compared with the result of Dennis *et al.*

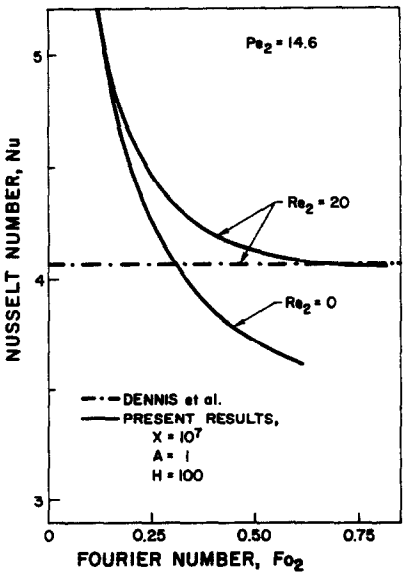

FIG. 2. Comparison of current results with that of Dennis *et al.* [7] for a solid sphere.

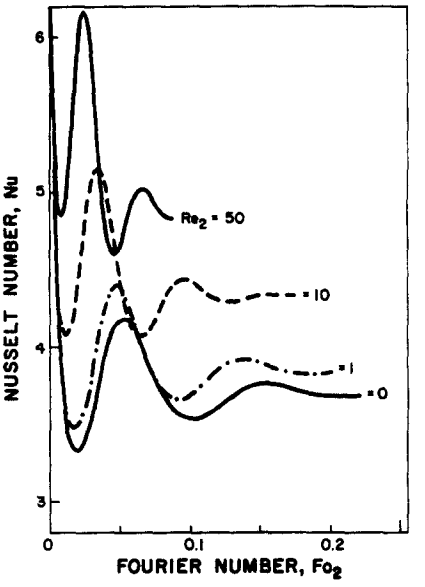

FIG. 4. Transient Nusselt number vs Fourier number for the case of $A = 1$, $B = 0.333$, $X = 0.333$ and $Pe_2 = 300$.

[7]. To simulate the external problem $H = 100$ and $A = 1$ were employed. With a finite value of H (rather than an infinite value of H), the Nusselt number predicted by the present method is expected to be slightly smaller than that for a pure external problem. The present results compare favorably with the theoretical solution of Dennis *et al.* (Fig. 2).

The present method has also been compared with the experimental investigation of Froessling [8]. Froessling [8] reported the local Nusselt number for sublimation of naphthalene into air with $Re_2 = 48$. The local Nusselt number is defined by

$$Nu_{loc} = -(2/Z_b)\left.\frac{\partial Z}{\partial r}\right|_{r=1}. \quad (35)$$

On Fig. 3 the local Nusselt number from Froessling [8] and that predicted by the present model for $Re_2 = 48$, $B = 100$, $A = 1$ and $Pe_2 = 120$ is reported. The comparison is generally very favorable (Fig. 3).

Based on the reasonable comparison with both the theoretical investigation of Dennis *et al.* [7] and the experimental results of Froessling [8], it is assumed that the velocity profiles and the energy equation were correctly solved for the moderate Reynolds number conjugated heat transfer process.

5. RESULTS AND DISCUSSION

For a basic understanding, sample calculations were made to examine the role of each parameter in the heat transfer process. Figures 4–7 were prepared

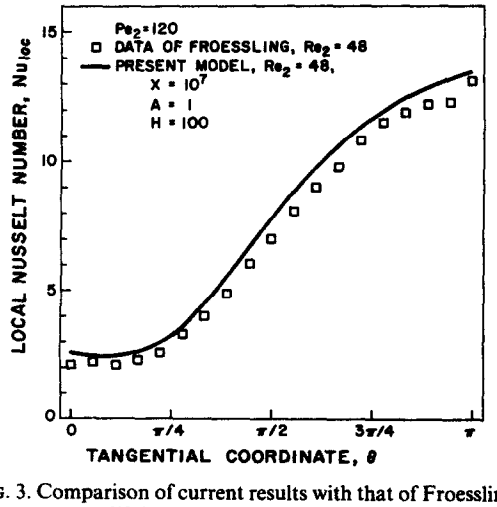

FIG. 3. Comparison of current results with that of Froessling [8] for local Nusselt numbers.

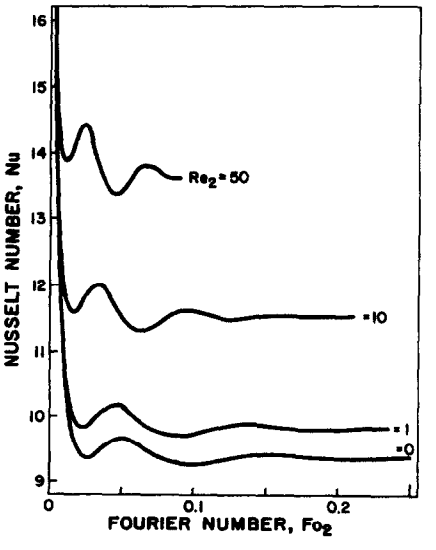

FIG. 5. Transient Nusselt number vs Fourier number for the case of $A = 1$, $B = 3$, $X = 0.333$ and $Pe_2 = 300$.

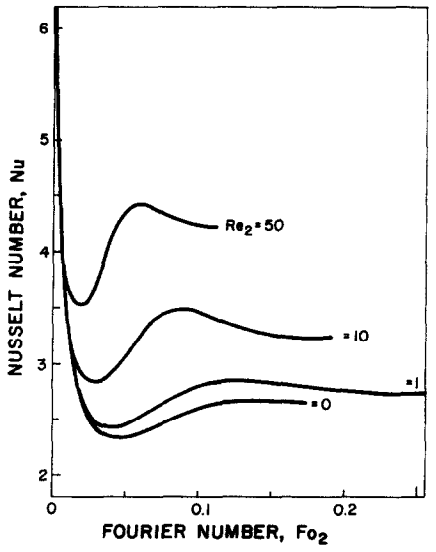

FIG. 6. Transient Nusselt number vs Fourier number for the case of $A = 1$, $B = 0.333$, $X = 3$ and $Pe_2 = 300$.

to show the effects of Reynolds number, dynamic viscosity ratio and thermal conductivity ratio in terms of the Nusselt number vs the Fourier number. For practical application purposes and the limitations of the current method, in Figs. 4–7 the Reynolds number, Re_2, was varied from 0 to 50, the dynamic viscosity ratio, X, from 0.333 to 3.0, and the thermal conductivity ratio, B, also from 0.333 to 3.0 for the parametric study. The thermal diffusivity ratio, A, is kept unchanged at unity and the Peclet number, Pe_2, is 300 for Figs. 4–7. As the Reynolds number increases, the strength of the internal circulation increases accordingly in a fluid sphere and so does the continuous phase velocity near the drop surface. This

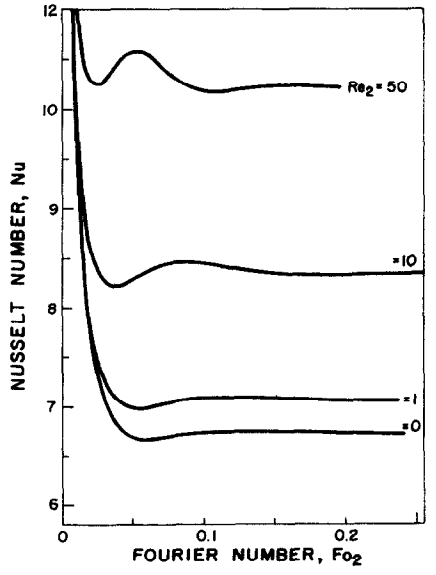

FIG. 7. Transient Nusselt number vs Fourier number for the case of $A = 1$, $B = 3$, $X = 3$ and $Pe_2 = 300$.

increased circulation with the corresponding increase in the ambient fluid velocity greatly enhances the rate of heat transport between the two phases. Consistently in all cases plotted in Figs. 4–7, the Nusselt number increases with the Reynolds number following similar trends. In general, the increased heat transfer with the Reynolds number is mainly due to an increase in the continuous phase velocity near the drop surface, whereas the increased internal circulation results in shorter oscillation cycles in the transient period.

Figures 4 and 5 show the effects of various thermal conductivity ratios, B, for $X = 0.333$. Two consistent trends are noticed. First, the Nusselt number increases with increasing B and second, the fluctuating amplitudes decrease with increasing B. The higher Nusselt number for increased B is because the Nusselt number is defined for heat transfer to the drop and higher internal thermal conductivity will result in a higher rate of heat diffusion from the surface to the interior of the fluid sphere and therefore the rate of heat transfer to the drop is increased. Higher internal thermal conductivity also enhances the rate of heat transfer from the drop surface to the center of the internal circulation instead of letting the thermal energy stay with the convective circulation loops that cause the fluctuations in Nusselt number. Therefore, the fluctuating amplitude is smaller as B is increased in the heat transfer process.

Figures 6 and 7 also show the effects of different B for a larger value of X, 3.0. Similar results are predicted as those for $X = 0.333$. Figures 4 and 6 demonstrate the effects of different dynamic viscosity ratio, X. When X becomes larger, the internal fluid is more viscous and this increase in viscosity causes the internal fluid to be more resistant to the induced internal circulation. Therefore, the strength of internal circulation is weaker for larger values of X. Reduction in internal circulation results in a longer oscillation cycle and a lower Nusselt number as shown in Figs. 4 and 6. Figures 5 and 7 also show the effects of variation of X. Similar conclusions may be made as those stated for Figs. 4 and 6.

Next we discuss two extreme cases, i.e. a solid sphere and a gas bubble.

For a solid sphere the conjugate heat transfer is less dependent on the Reynolds number, particularly at low values of B. For a solid sphere the interfacial velocity is always zero, thus there is no increase in the continuous phase velocity near the sphere surface due to an increased circulation in the sphere. Also the internal resistance is always due to pure diffusion, thus the increase in transfer rates that correspond to the increase in internal circulation will not be realized for a solid sphere. The predicted Nusselt numbers are plotted for the special cases of $B = 0.333$, 1.0 and 3.0 for $A = 1$, $X = 10^7$, $Re_2 = 20$ and $Pe_2 = 300$ in Fig. 8. The Nusselt numbers using the same thermal parameters (B, A, Pe_2), with the creeping flow velocities are also included in Fig. 8 for comparison purposes.

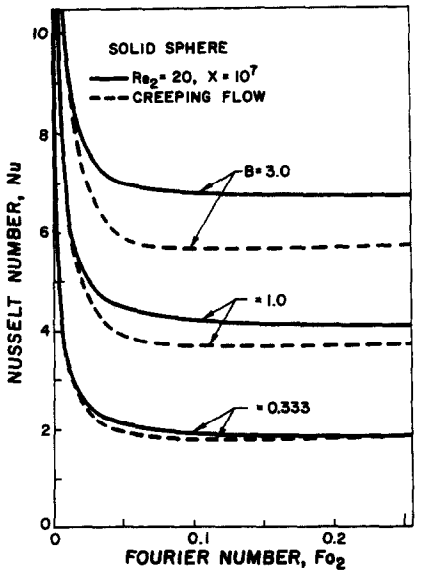

FIG. 8. Transient Nusselt number vs Fourier number for a solid sphere ($X = 10^7$) with $A = 1$, and $Pe_2 = 300$ at various B of 0.333, 1 and 3.

It is noted that for low B, the external flow variations do not change the heat transfer significantly. This is because at low B, the heat transfer resistance is mostly with the interior of the solid sphere, any decrease in external resistance due to increased convection only alters the conjugate heat transfer slightly.

For a gas bubble ($X = 0$), the Nusselt number vs the Fourier number plots for Reynolds numbers of 0 and 10 are given in Fig. 9. For a gas bubble, the strength of the internal circulation is always a maximum for a given Reynolds number. Because of

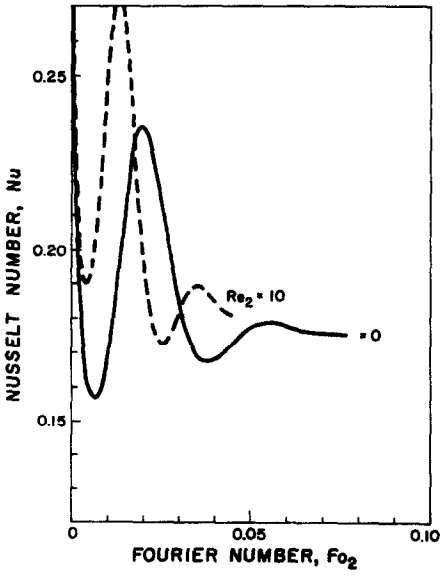

FIG. 9. Transient Nusselt number vs Fourier number for a gas bubble ($X = 0$) with $A = 2$, $B = 0.01$ and $Pe_2 = 640$ at Reynolds numbers of 0 and 10.

Table 1. Comparison of equation (36) with the present results for the asymptotic Nusselt number for a solid sphere with $Pe_2 = 300$ and $Re_2 = 20$

B	Nu_{asy} Equation (36)	Nu_{asy} Present results
0.333	1.78	1.84
1.0	3.89	4.08
3.0	6.41	6.72

the corresponding extremely low B value, the heat transfer resistance is almost totally with the bubble. Any increase in Reynolds number only increases the amplitude of the fluctuations and the frequency during the transient, but the steady-state Nusselt number is nearly independent of the Reynolds number.

It is instructional to revisit equation (30) of ref. [1]. This equation was shown to be useful in predicting the steady-state Nusselt number for conjugate heat transfer for the special case of $A = 1$

$$Nu_{asy} \simeq \left[\frac{1}{B\,Nu_{int}} + \frac{1}{Nu_{ext}}\right]^{-1}. \tag{36}$$

The internal Nusselt number for pure diffusion is given by

$$Nu_{int} = 6.58. \tag{37}$$

For solid spheres, the external Nusselt number may be reasonably approximated using equation (5-25) of Clift *et al.* [9]

$$Nu_{ext} = 1 + [1 + Pe_2^{-1}]Pe_2^{0.333}\,Re_2^{0.08}. \tag{38}$$

For the cases investigated above, with $Re_2 = 20$, $Pe_2 = 300$ the resulting value of Nu is 9.5. The Nusselt numbers predicted by equation (36) are compared with the present results in Table 1. As with low Reynolds numbers, equation (36) appears to predict the asymptotic Nusselt number with reasonable accuracy for conjugate heat transfer from solid spheres for moderate Reynolds numbers.

6. CONCLUSION

The conjugate heat transfer from drops and solid spheres has been investigated for moderate Reynolds numbers. For fluid drops, it was found that the increased velocities near the interfacial surface of a drop as a result of an increase in the Reynolds number also enhances the rate of conjugate heat transfer from the drop.

The conjugate heat transfer from solid spheres appears to be less sensitive to the change in the Reynolds number. Also equation (36) was found to predict reasonably well the asymptotic value of the Nusselt number for conjugate heat transfer for $Re_2 = 20$ if the thermal diffusivities of the two phases are equal.

REFERENCES

1. D. L. R. Oliver and J. N. Chung, Conjugate unsteady heat transfer of a translating droplet at low Reynolds number, *Int. J. Heat Mass Transfer* **29**, 879–887 (1986).
2. F. Cooper, Heat transfer from a sphere to an infinite medium, *Int. J. Heat Mass Transfer* **20**, 991–993 (1976).
3. B. M. Abramzon and I. Borde, Conjugate unsteady heat transfer from a droplet in creeping flow, *A.I.Ch.E. Jl* **26**, 536–544 (1980).
4. B. T. Chao, Transient heat and mass transfer to a translating drop, *J. Heat Transfer* **91**, 273–281 (1969).
5. M. D. Van Dyke, A model of series truncation applied to some problem in fluid mechanics, Stanford University Report SUDAER 247 (1965).
6. D. L. R. Oliver and J. N. Chung, Flow about a fluid sphere at low to moderate Reynolds numbers, *J. Fluid Mech.* **177**, 1–18 (1987).
7. S. C. R. Dennis, J. D. A. Walker and J. D. Hudson, Heat transfer from a sphere at low Reynolds number, *J. Fluid Mech.* **60**, 273–283 (1973).
8. N. Froessling, Uber die Verdunstung Fallender Tropfen, *Gerlands Beitr. Geophysics* **52**, 170–216 (1938).
9. R. Clift, J. R. Grace and M. E. Weber, *Bubble, Drops and Particles*, Academic Press, New York (1978).

TRANSFERT THERMIQUE VARIABLE CONJUGUE POUR UNE SPHERE FLUIDE EN TRANSLATION A DES NOMBRES DE REYNOLDS MODERES

Résumé—On étudie numériquement le transfert thermique variable et conjugué entre une gouttelette en translation et son environnement fluide, à des nombres de Reynolds modérés. L'équation d'énergie est résolue par une méthode ADI de différences finies, avec mouvements de fluide, à l'intérieur et à l'extérieur de la gouttelette, simulés par une méthode spectrale à série tronquée. Le domaine des nombres de Reynolds est compris entre 0 et 50. Les rapports des viscosités et des conductivités thermiques de la goutte et du fluide ambiant varient respectivement de 0 à 10^7 et de 0,01 à 3. On trouve que l'accroissement du nombre de Reynolds s'accompagne d'une augmentation du transfert qui résulte des mouvements accrus à l'intérieur comme à l'extérieur de la gouttelette. D'autre part, le flux transféré pour une sphère solide est moins sensible au nombre de Reynolds que pour une sphère fluide. Pour une bulle de gaz, un accroissement quelconque du nombre de Reynolds augmente seulement l'amplitude et la fréquence des fluctuations dans le nombre de Nusselt alors que le nombre de Nusselt de régime permanent est à peu près indépendant du nombre de Reynolds.

INSTATIONÄRER KONJUGIERTER WÄRMEÜBERGANG AN EINER SICH BEWEGENDEN FLUIDEN KUGEL BEI MITTLEREN REYNOLDS-ZAHLEN

Zusammenfassung—Der instationäre Wärmeübergang zwischen einem bewegten Tröpfchen und dem umgebenden Fluid wird für mittlere Reynolds-Zahlen numerisch untersucht. Die Energiegleichung wird mit Hilfe des ADI-Finite-Differenzen-Verfahrens mit Flüssigkeitsbewegungen außerhalb und innerhalb des Tröpfchens gelöst, die durch ein Reihen-Abbruchs-Spektralverfahren simuliert werden. Der Bereich der untersuchten Reynolds-Zahlen reicht von 0 bis 50. Das Verhältnis der Viskositäten und der Wärmeleitfähigkeiten von Tröpfchen und umgebender Strömung reicht von 0 bis 10^7 beziehungsweise 0,01 bis 3. Durch Erhöhen der Reynolds-Zahl wird der berechnete Wärmeübergang für fluide Kugeln wesentlich verbessert. Dies ist auf zunehmende Fluidbewegungen innerhalb und außerhalb des Tröpfchens zurückzuführen. Andererseits ist der Wärmeübergang an feste Kugeln weit weniger von der Reynolds-Zahl abhängig als bei fluiden Kugeln. Für eine Gasblase führt jedes Anwachsen der Reynolds-Zahl nur zum Anstieg der Amplitude und der Frequenz der Schwankungen in der Nusselt-Zahl, die stationäre Nusselt-Zahl ist fast unabhängig von der Reynolds-Zahl.

НЕСТАЦИОНАРНЫЙ СОПРЯЖЕННЫЙ ТЕПЛОПЕРЕНОС ОТ ЖИДКОЙ СФЕРЫ ПРИ УМЕРЕННЫХ ЧИСЛАХ РЕЙНОЛЬДСА

Аннотация—Численно исследуется сопряженный нестационарный теплоперенос между движущейся каплей и окружающей ее жидкостью при умеренных числах Рейнольдса. Уравнение сохранения энергии решается с помощью неявной разностной схемы методом переменных направлений, причем движение жидкости внутри капли и вне ее моделируется конечным числом членов спектрального ряда. Исследования проводятся в диапазоне значений числа Рейнольдса 0–50. Отношения вязкости и коэффициентов теплопроводности капли и окружающего ее потока изменяются соответственно от 0 до 10^7 и от 0,01 до 3. Найдено, что с увеличением числа Рейнольдса расчетное значение скорости теплопереноса для жидких сфер существенно возрастает в результате интенсификации движения жидкости как внутри капли, так и снаружи. При обтекании твердой сферы скорость теплопереноса намного меньше зависит от числа Рейнольдса, чем для жидких сфер. В случае пузырька газа увеличение числа Рейнольдса вызывает лишь рост амплитуды и частоты колебаний мгновенного числа Нуссельта, а стационарное число Нуссельта почти не зависит от числа Рейнольдса.